A Comparison of Forecast Errors in CAM2 and CAM3 at the ARM Southern Great Plains Site

DAVID L. WILLIAMSON AND JERRY G. OLSON

National Center for Atmospheric Research,* Boulder, Colorado

ABSTRACT

The authors compare short forecast errors and the balance of terms in the moisture and temperature prediction equations that lead to those errors for the Community Atmosphere Model versions 2 and 3 (CAM2 and CAM3, respectively) at T42 truncation. The comparisons are made for an individual model column from global model forecasts at the Atmospheric Radiation Measurement Program (ARM) Southern Great Plains site for the April 1997 and June–July 1997 intensive observing periods. The goal is to provide insight into parameterization errors in the CAM, which ultimately should lead to improvements in the way processes are modeled. The atmospheric initial conditions are obtained from the 40-yr ECMWF Re-Analysis (ERA-40). The land initial conditions are spun up to be consistent with those analyses. The differences between the model formulations that are responsible for the major differences in the forecast errors and/or parameterization behaviors are identified. A sequence of experiments is performed, accumulating the changes from CAM3 back toward CAM2 to demonstrate the effect of the differences in formulations.

In June–July 1997 the CAM3 temperature and moisture forecast errors were larger than those of CAM2. The terms identified as being responsible for the differences are 1) the convective time scale assumed for the Zhang–McFarlane deep convection, 2) the energy associated with the conversion between water and ice of the rain associated with the Zhang–McFarlane convection parameterization, and 3) the dependence of the rainfall evaporation on cloud fraction. In April 1997 the CAM2 and CAM3 temperature and moisture forecast errors are very similar, but different tendencies arising from modifications to one parameterization component are compensated by responding changes in another component to yield the same total moisture tendency. The addition of detrainment of water in CAM3 by the Hack shallow convection to the prognostic cloud water scheme is balanced by a responding difference in the advective tendency. A halving of the time scale assumed for the Hack shallow convection was compensated by a responding change in the prognostic cloud water. Changes to the cloud fraction parameterization affect the radiative heating, which in turn modifies the stability of the atmospheric column and affects the convection. The resulting changes in convection tendency are balanced by responding changes in the prognostic cloud water parameterization tendency.

1. Introduction

The Community Atmosphere Model version 3 (CAM3), developed in a collaboration between members of the National Center for Atmospheric Research and the scientific research community, was recently released for unrestricted use by the general community.

The CAM3 is the atmospheric component of the new version of the Community Climate System Model (CCSM3), which is intended for coupled ocean–atmosphere–sea ice applications, including climate change studies such as those carried out for the Intergovernmental Panel on Climate Change (IPCC). The CCSM3 is documented in Collins et al. (2006a) and in a series of papers in a special issue of the *Journal of Climate* (2006, Vol. 19, No. 11).

The CAM3 can also be run in a stand-alone mode with specified sea surface temperatures (SSTs) and sea ice extent while coupled with the Community Land Model (CLM; Bonan et al. 2002a; Oleson et al. 2004). A complete technical description of CAM3 is provided by Collins et al. (2004). It is closely related to its prede-

cessor CAM2 (Collins et al. 2003; Kiehl and Gent 2004), with a few of its component parameterizations essentially unchanged. Nevertheless, extensive modifications have been introduced into the cloud and precipitation processes and are described in Boville et al. (2006), Zhang et al. (2003), and Collins et al. (2006b).

Many of the formulation changes were introduced to eliminate significant biases in the climate simulated by CAM2, which limited its utility for several applications (e.g., see Boville et al. 2006). As part of the development and evaluation of CAM3, adjustable coefficients in the parameterization of clouds and precipitation were also modified. Hack et al. (2006a) provide an overview of the need to "tune" adjustable parameters in response to changes in large-scale fields that can accompany parameterized forcing and resolution changes.

As alluded to above, the CAM3 was developed by comparing its simulated climate to similar statistics obtained from atmospheric observations and analyses, with the goal of matching the atmospheric statistics as closely as possible. In fact CAM3, although not perfect, provides a better match than CAM2 did, indicating that the design criteria were largely satisfied. Many of the improvements in the climate statistics of the simulations are described in Collins et al. (2006a,b), Boville et al. (2006), Hack et al. (2006b), and Rasch et al. (2006). Hurrell et al. (2006) describe the overall dynamical simulation of the CAM3. All these papers and others in the *Journal of Climate* special issue indicate that the simulated climate of CAM3 is an improvement over that produced by its predecessor CAM2. While all these papers concentrate on improvements to the simulated climate they also list important remaining biases that reduce the fidelity of CAM3 simulations.

2. Description of forecast approach

As indicated above, CAM3 does a credible job of simulating current climate; however, for it to be most useful it must do so by correctly approximating the processes that create that climate. Evaluation of those processes when the model is in its climate equilibrium may be misleading because a process might be responding to or creating compensating errors. In addition, evaluation of the modeled processes is difficult and perhaps not possible on a global scale. However, with colleagues at the Program for Climate Model Diagnosis and Intercomparison (PCMDI) we have developed an approach to examine the processes in climate models by following the lead of NWP model development, that is, to examine the climate model applied to weather forecasts. The goal is not to produce the best possible forecast or to determine the longer-term evolution of the

forecast error, but rather to compare model-parameterized variables such as clouds and radiation and parameterized tendencies to detailed estimates from field campaigns such as those provided by the Department of Energy (DOE) Atmospheric Radiation Measurement (ARM) program. Such comparisons can only be made in limited regions and for limited periods, but they do shed light on how the models are working there. The parameterizations are examined when they are applied to the observed atmospheric state rather than to a possibly incorrect model-simulated state. Our general approach, which has been named the Climate Change Prediction Program (CCPP)-ARM Parameterization Test Bed (CAPT) is described in Phillips et al. (2004). We emphasize that our goal is to gain insight into model parameterization errors, which we hope will lead to suggestions for model improvements. Boyle et al. (2005) and Williamson et al. (2005) apply the approach to CAM2 for a few periods and locations. The argument is that when the parameterizations are applied to the correct atmospheric state, as provided by high-resolution numerical weather prediction analysis systems, initial errors in the forecasts are attributable to the parameterizations. Of course it must be affirmed that the dynamical component is accurate during the period being analyzed. This approach also concentrates on the errors that have the fastest time scales. After these fast errors are established, the model state is no longer a good estimate of the atmosphere and our original assumption that the parameterizations are applied to the correct atmospheric state is no longer valid. We will see below that the errors form very rapidly in the cases considered here. One can consider the longer-term evolution and balance of the errors (e.g., Sud et al. 2006), but once the model state differs from the atmospheric state we have a similar problem as looking at the individual processes in the climate equilibrium described above.

In this paper we compare forecasts made by CAM3 to matching ones made by CAM2 at the ARM Southern Great Plains (SGP) site for the April 1997 and June–July 1997 intensive observing periods (IOPs). Both versions were run at T42 spectral truncation with 26 vertical levels. We do not catalog the details of all the differences between CAM2 and CAM3. Similarly, we do not identify the effect of all those differences between CAM2 and CAM3 on the errors in the modeled processes or in the balances between processes. Rather we identify the primary differences between the model formulations that are responsible for the major differences in the forecast errors and/or parameterization behavior. As will be seen, these involve the changes in the values of some parameters, changes in

the details of some parameterizations, and the inclusion of additional processes in CAM3.

Williamson et al. (2005) showed that for these periods and locations the primary CAM2 forecast errors form rapidly within 24 h. For the next several days the errors evolve slowly as the errors with slower time scales respond to the early errors. We have found that the errors in CAM3 are similar to those in CAM2 and form equally rapidly. Therefore we consider the temperature and specific humidity errors of 24-h forecasts and the terms in the temperature and moisture prediction equations averaged over the first 24 h of the forecasts. In addition, to reduce the noise we consider composite forecast errors rather than the errors of individual forecasts. The composites are chosen to consist of forecasts with common errors and behavior as in Williamson et al. (2005). The rationale given there for CAM2 applies equally to the CAM3 forecasts. The analyses of individual forecasts are very similar to that of the composite.

The specific humidity and thermodynamic prognostic equations can be written

$$\frac{\partial q}{\partial t} = -\mathbf{V} \cdot \nabla q - \dot{\sigma} \frac{\partial q}{\partial \sigma} + S, \qquad (1)$$

$$\frac{\partial T}{\partial t} = -\mathbf{V} \cdot \nabla T - \dot{\sigma} \frac{\partial T}{\partial \sigma} + \kappa T \frac{\omega}{p} + Q, \qquad (2)$$

where the moisture source term S and heating term Q represent the subgrid-scale parameterizations. The first two terms on the right-hand sides of (1) and (2) denote the horizontal and vertical advection. We also consider the sum of these two—referred to as the total advection. We refer to the term $\kappa T \omega / p$ in (2) as the energy conversion term since the momentum equation includes a corresponding term and the global integrals of the two sum to zero in the total energy equation.

For the purposes of identification in the following analysis of differences we define here the terms we will use to characterize the various processes examined. In general, we separate the parameterizations, S and Q, into three primary components referred to as the moist processes parameterization, the planetary boundary layer (PBL) parameterization, and radiation. The last has no direct effect on the moisture source term S. The PBL parameterization includes the surface fluxes that are distributed in the vertical by the PBL parameterization (Holtslag and Boville 1993). The moist processes include the Zhang and McFarlane (1995) deep convection parameterization, the Hack (1994) shallow convection parameterization, and a prognostic cloud water parameterization (Rasch and Kristjansson 1998). These three can be thought of as creating condensate or

rainwater from water vapor. We refer to these as the primary parameterization schemes included in the moist processes, but each has complementary processes associated with it that act on the condensate produced by its corresponding primary parameterization. These processes include the evaporation of falling rainwater created by the prognostic cloud water, by the Zhang–McFarlane deep convection parameterization, and by the Hack shallow parameterization. We refer to these as rainfall evaporation. In CAM2 there is no rainfall evaporation associated with the Hack shallow parameterization. CAM2 includes a term associated with the Zhang–McFarlane deep convection parameterization that evaporates a fraction of the detrained water back into the environment. We refer to this as environmental detrainment. This term is not included in CAM3. Additional processes included in CAM3 that are not included in CAM2 are the partitioning of condensate into liquid and ice, the freezing of rainwater to snow or ice, and the inverse melting of snow or ice back to rainwater. These are associated with each of the three primary parameterizations of the moist processes and all follow the formulation of Rasch and Kristjansson (1998). They provide an energy consistency in CAM3 that was lacking in CAM2.

We use the same atmosphere and land initial conditions for CAM3 as were used for CAM2 in Boyle at al. (2005) and Williamson et al. (2005) with minor modifications to the land conditions required by minor differences in the land models. These will be described shortly. The initial atmospheric conditions were obtained by mapping high-resolution 40-yr European Centre for Medium-Range Weather Forecasts (ECMWF) Re-Analysis (ERA-40; Simmons and Gibson 2000) to the coarse-resolution CAM grid in a way that is consistent with the low-resolution topography, and leads to smooth, balanced forecasts. We followed the interpolation method used in the IFS system jointly developed by the ECMWF and Meteo-France (White 2001). In the earlier CAM2 study we also used initial conditions created from the National Centers for Environmental Prediction (NCEP)–DOE reanalyses (R2; Kanamitsu et al. 2002). The general characteristics of the forecast errors from the two sets of initial conditions were the same, although the magnitudes of the errors differed somewhat. By comparison with the independent ARM data at the SGP site, we concluded that the ERA-40 initial conditions provided a truer indication of the CAM error.

The land initial conditions for the CLM2 that was coupled to CAM2 were obtained by a spinup procedure in which the CLM2 responds to and interacts with the CAM2 while the CAM2 is forced with the ERA-40

analyses to evolve like the observed atmosphere. This is described in more detail in Phillips et al. (2004) and in Boyle et al. (2005). Some indication of the quality of the land initial conditions is provided in Boyle et al. (2005) and Williamson et al. (2005) where it is argued that any deficiencies in the land initial conditions are not responsible for the primary errors seen in those papers in the atmospheric forecasts. By analogy, they are not responsible for the errors seen with CAM3 either. The CLM2 was based on a grid box containing multiple plant function types, each with its own soil column. The CLM3 includes the effects of competition for water among plant function types by having a single soil column shared by all the plant function types within a grid box (Bonan et al. 2002a; Oleson et al. 2004). For the CLM3/CAM3 forecasts considered in the following we set the initial soil column in each grid box to match the initial CLM2 column of the dominant plant function type. We also carried out CLM3/CAM3 forecasts using the average of the CLM2 soil columns in each grid box weighted by plant-type fraction, and using the original CAM2 initial data with CLM3 set in noncompete mode with multiple soil columns in the grid box. The differences between the resulting CAM3 forecasts were minimal.

The prognostic parameterized variables, that is, those variables that carry information from one time step to the next, were initialized in the spinup procedure used for the land. The only modification to the CAM2 variables needed for CAM3 was to partition the total condensate into liquid and ice forms. The algorithm included in the CAM2 prognostic cloud water scheme (Rasch and Kristjansson 1998) was used. We note that these initial values play a minor role in the forecasts since they are very close to what CAM3 would produce in a similar spinup exercise, and even if not initialized they spin up in forecasts to their preferred values extremely fast.

We emphasize that we consider only two specific seasons (April and June–July 1997) at an individual grid column, namely, the ARM SGP site. However, the April case does appear to be representative of other years (Boyle et al. 2005), and the June–July errors might be relevant to the model behavior in other moist regions such as the tropical western Pacific (Williamson et al. 2005). The analyses presented here are not necessarily representative of the model's behavior everywhere. Nevertheless, they do shed some light on the workings of some of the parameterizations.

We calculate the model errors by comparing with the ARM IOP datasets that were developed for forcing and diagnosing single-column and cloud-resolving models. These have been processed with the constrained varia-

tional analysis method of Zhang and Lin (1997) and Zhang et al. (2001). These data include the variables needed to drive single-column models (SCMs) and additional fields such as estimates of the subgrid-scale forcing equivalent to what would be calculated by a model parameterization suite. These are obtained as a residual of the total tendency minus the advective or dynamical terms. We emphasize, however, that we are not studying an SCM here. Our analysis is for an individual column, from global forecasts of the complete model so that interactions with the active dynamical component are included.

To illustrate the changes in model formulation that we have identified as responsible for the major differences between the CAM2 and CAM3 forecast errors we start with the CAM3 formulation and modify selected aspects to match those of CAM2. We perform a sequence of experiments, accumulating the changes from CAM3 back toward CAM2. Each set of forecasts in the sequence will be referred to as an "experiment."

3. June–July 1997 IOP forecasts

Williamson et al. (2005) showed that the dominant errors in CAM2 in June–July at the SGP site were persistent, occurring in every forecast. Therefore we average over all forecasts for this period as was done in the analysis of Williamson et al. (2005). Figures 1a,b show the vertical profiles of the mean forecast temperature and specific humidity errors at day 1 for CAM3 (solid line) and CAM2 (short dashed line) at the ARM SGP site. The data are vertically interpolated to a common grid consisting of the union of the CAM and ARM grids to compute the error. The inner tick marks on Figs. 1a,b indicate the interpolation grid at which the differences are plotted. The CAM2 values in Figs. 1a,b replicate the corresponding DAY 1 curves in Fig. 1 of Williamson et al. (2005). The long dashed line is from the first in the sequence of experiments and will be discussed shortly. The CAM3 errors are larger than the CAM2 errors at this location and season. Corresponding profiles of CAM3 and CAM2 June–July simulation climatological errors at this grid point are shown in Figs. 1c,d. Here the data are vertically interpolated to a common grid consisting of the union of the CAM and ERA-40 grids to compute the error. The inner tick marks indicate these points. The climatological errors are calculated from a 21-yr simulation with monthly averaged sea surface temperatures differenced against ERA-40 averaged over the same period. The larger CAM3 upper-tropospheric forecast temperature error is reflected in the CAM3 climatological error also being larger than that of CAM2. CAM2 has a larger lower-
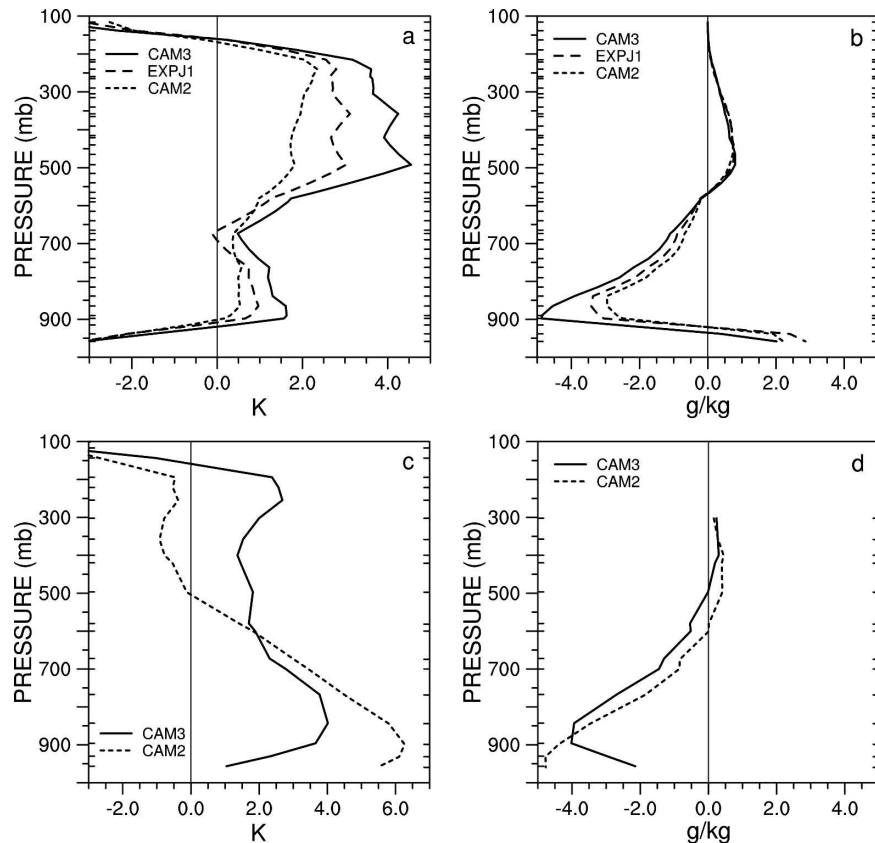
FIG. 1. Mean day-1 forecast (a) temperature and (b) specific humidity errors for CAM3 (solid), EXPJ1 (long dash), and CAM2 (short dash) for the June–July 1997 IOP. Mean CAM3 and CAM2 climate (c) temperature and (d) specific humidity errors for June–July. All at the ARM SGP site.

tropospheric climatological temperature error because the land model develops a warm, dry bias (Bonan et al. 2002b) in the summer. This error develops in the climate simulation on a longer time scale than the short forecasts considered here. The CAM3 climatological moisture bias is also larger than that of CAM2 except near the surface where the CAM2 land dry bias affects the atmospheric climatology. Again the land climatological bias sets up over a longer period than the few-day forecasts considered here. Clearly the 1-day forecast errors are not identical to the climate biases, but the CAM forecast biases do appear to be relevant to the climatological biases. The 1-day forecast errors represent only those that form fastest while additional errors come into play in the climate simulation. After they form, these slower errors probably partially ameliorate the fastest errors reducing the climate bias. In addition, the forecast error is for a composite of cases from mid-June to mid-July for a single year. The composite is chosen to consist of only forecasts that have the same forecast error. The climate bias is for the entire 2 months for multiple years. There is a greater possibility of mixing different types of errors in creating the climate average.

Williamson et al. (2005) show that the moist processes are driving most of the temperature error in the CAM2 forecasts at this season, and within that set of processes, the Zhang–McFarlane deep convection parameterization is dominant, the others being relatively inactive. Of course, as pointed out there, the formulation of the parameterization might not be in error. It might be responding to errors in other processes. Nevertheless, it is a good starting point to attempt to understand the sources of the errors, or differences in the errors that are indicated here. We have identified three changes from CAM2 to CAM3 associated with the Zhang–McFarlane deep convection that are responsible for most of the difference in the forecast errors. These are 1) parameters in the deep convection were modified to make it more active in CAM3, 2) the energy associated with the conversion between water and ice of the convective rain was added to CAM3, and 3) the rainfall evaporation in CAM3 was made to depend in the cloud fraction.
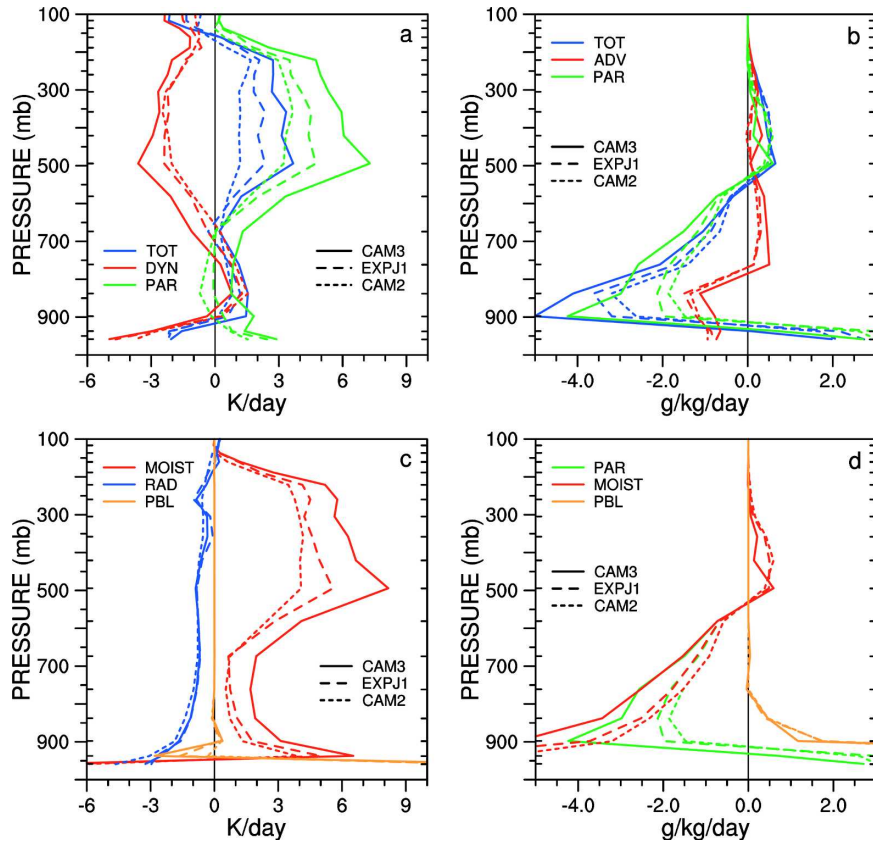
FIG. 2. Mean forecast 0–24-h average of terms in the temperature and specific humidity prediction equation for the June–July 1997 IOP: (a) temperature tendencies; (b) specific humidity tendencies; (c) temperature tendencies; and (d) specific humidity tendencies.

We now discuss a sequence of experiments accumulating the reverse of these changes from CAM3 back toward CAM2 to demonstrate that they are indeed responsible for most of the observed forecast differences. The experiments are summarized in Table 1.

In the first experiment, labeled EXPJ1, the time scale for the Zhang–McFarlane deep convection is increased from the CAM3 value of 1 h to the CAM2 value of 2 h [Eq. (4.42) of Collins et al. 2004]. The time-scale difference makes the convection less active in EXPJ1 than in CAM3. In addition, the coefficient controlling the autoconversion of cloud water to precipitation as it is lifted is decreased from 3×10^{-3} m^{-1} in CAM3 to the CAM2 value of 2×10^{-3} m^{-1} [Eq. (4.20) of Collins et al. 2004]. The decrease in the autoconversion coefficient in EXPJ1 results in less rainwater being produced. The errors in the EXPJ1 forecasts are compared to

those of CAM3 and CAM2 in Figs. 1a,b as the long dashed line. The temperature error from EXPJ1 falls halfway between CAM3 and CAM2 values except around 700 mb where the error is less than that of CAM2. The moisture error is two-thirds of the way from CAM3 to CAM2, with no particularly noticeable feature at 700 mb. A separate set of forecasts changing only the convective time scale from the CAM3 to the CAM2 value (not shown) shows that the changes from CAM3 to EXPJ1 seen in Figs. 1a,b are primarily due to the convective time-scale change and not to the change in autoconversion coefficient.

Figures 2a,b show the 24-h-averaged total temperature and moisture tendencies (TOT) along with their two components, the dynamics (DYN) or advection (ADV) tendencies, and the parameterization tendencies (PAR), for the CAM3, CAM2, and EXPJ1. The

TABLE 1. Sequence of experiments for June–July 1997 with accumulated changes from CAM3 back to CAM2.

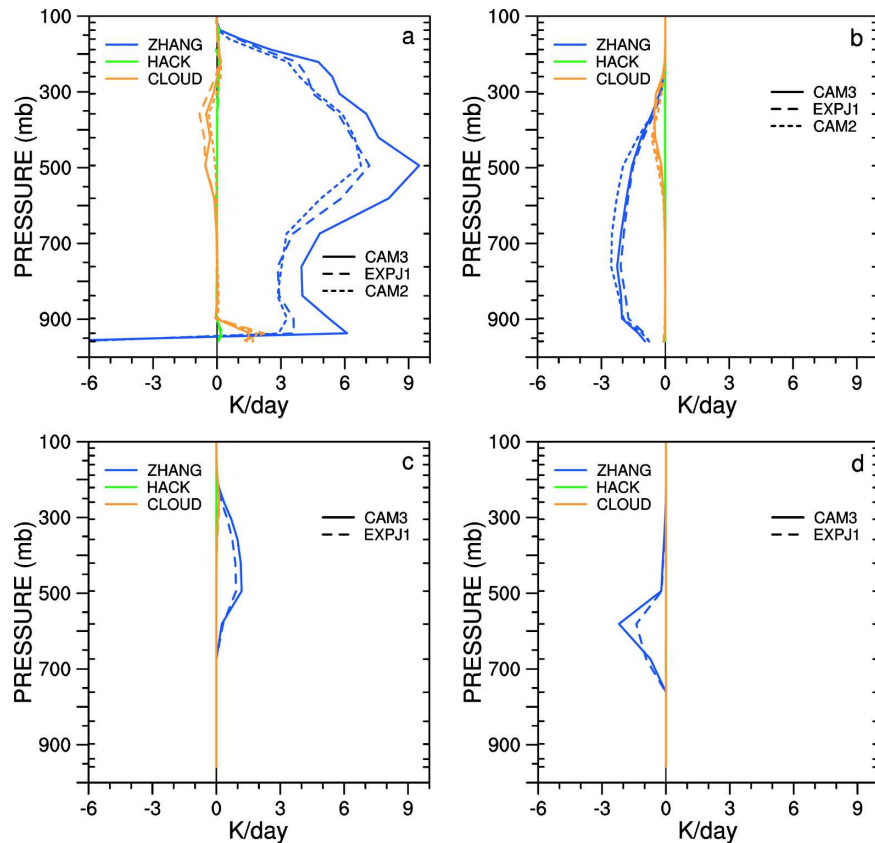|	
EXPJ1	CAM3 with Zhang convective time scale and autoconversion coefficient set to CAM2 values
EXPJ2	EXPJ1 with conversion between water and ice associated with convective parameterization eliminated
EXPJ3	EXPJ2 with $(1 - C_f)$ term eliminated from rainfall evaporation

FIG. 3. Mean forecast 0–24-h average temperature tendencies for CAM3, EXPJ1, and CAM2 for the June–July 1997 IOP: (a) formation of condensate, (b) rainfall evaporation, (c) freezing of rainwater, and (d) melting of snow, each associated with Zhang–McFarlane deep convection (ZHANG), Hack shallow convection (HACK), and prognostic cloud parameterization (CLOUD).

inner tick marks indicate the actual model levels. The dynamics cools more in CAM3 than CAM2 throughout the column (Fig. 2a). Presumably the dynamics is responding to differences caused by the parameterizations during the first day since the dynamical approximations are identical in CAM2 and CAM3, and the initial data and surface boundary data are nearly the same. In fact, examinations of 3-h averages shows that the dynamics and moisture advection in CAM3 match those of CAM2 during the part of the day when the convection is inactive (6–15 h). The differences in temperature and moisture created by the parameterizations during the first 6 h are not large enough to affect the dynamics and advection from 6 to 15 h. The dynamics and advection differences then grow from 15 to 24 h when the convection is active. The convection gives a different heating rate, which in turn drives a different vertical motion. The differences in the dynamics are in fact in the vertical advection and energy conversion term. The horizontal advection matches in the CAM2 and CAM3 forecasts. This was further verified by ex-

amining sets of forecasts initialized at 0600 and 1200 UTC. The dynamics and moisture advection match in the two sets of forecasts before the convection is activated. The dynamical tendency in EXPJ1 with the convective time scale set to CAM2 values is closer to that of CAM2 (Fig. 2a), consistent with the state being closer to that of CAM2. However, the parameterized heating and moistening still differ between EXPJ1 and CAM2. Williamson et al. (2005) compared the CAM2 parameterized moistening to that from the ARM variational dataset. This showed significant errors in CAM2 that are exacerbated in CAM3. Figures 2c,d indicate that the differences in temperature and specific humidity are primarily caused by the moist processes, with a very small contribution to the temperature tendency from the radiation.

Figure 3a shows the temperature tendency for the three primary parameterization schemes comprising the moist processes that create condensate. Figures 3b,c,d show the additional processes associated with each of the primary schemes. Figure 3a represents the
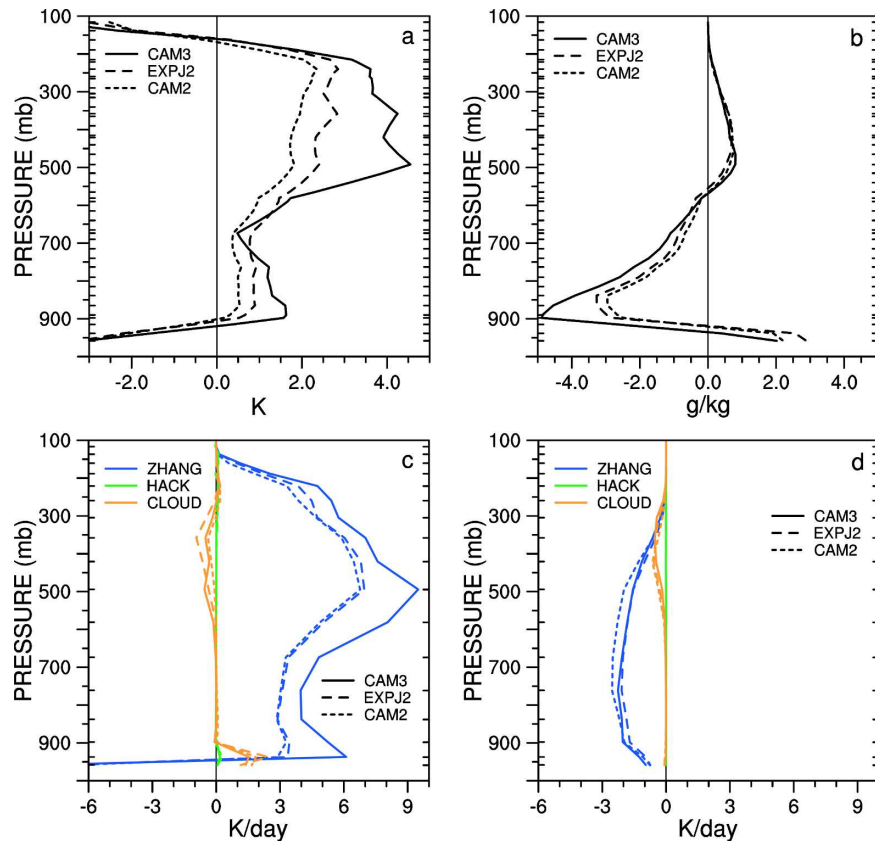
FIG. 4. Mean day-1 (a) forecast temperature and (b) specific humidity errors for CAM3, EXPJ2, and CAM2 for the June–July 1997 IOP. Mean forecast 0–24-h average temperature tendencies from (c) formation of condensate and (d) rainfall evaporation associated with Zhang–McFarlane deep convection (ZHANG), Hack shallow convection (HACK), and prognostic cloud parameterization (CLOUD).

conversion of vapor to liquid condensate in the case of the prognostic cloud water scheme and to rain or detrained water for the Zhang–McFarlane deep and Hack shallow convection parameterization. The Zhang–McFarlane deep convection is the dominant component and EXPJ1 is close but not identical to CAM2. Figure 3b shows the rainfall evaporation associated with the three parameterizations for the three experiments. CAM2 did not include rainfall evaporation with the Hack shallow scheme, but that term is also essentially zero in CAM3 and EXPJ1 and is not responsible for the differences. The rainfall evaporation is relatively small for the prognostic cloud water scheme. The rainfall evaporation associated with the Zhang–McFarlane deep convection dominates the three and for it, EXPJ1 is closer to CAM3. Figure 3c shows heating due to the freezing of rainwater to ice or snow associated with each scheme. This is essentially the ice–liquid repartitioning for the prognostic cloud water scheme with a similar repartitioning applied to the rainwater pro-

duced by the two convection schemes. Figure 3d shows the cooling due to the melting of snow for each scheme. These last two processes involving liquid–ice conversions were not included in CAM2 for any of the primary parameterizations. Figures 3c,d show that these conversion terms are small for the Hack shallow and prognostic cloud water parameterizations and that the conversions associated with the Zhang–McFarlane deep convection scheme dominate. The tendencies of EXPJ1 remain close to those of CAM3 as opposed to zero in CAM2.

Experiment EXPJ2 is based on EXPJ1 with the conversion between water and ice associated with the convection parameterizations eliminated. This conversion that was added to CAM3 for convective condensate follows the form used with the prognostic cloud formulation [Eqs. (4.114)–(4.143) of Collins et al. 2004]. Results are shown in Fig. 4. Comparison of EXPJ2 in Fig. 4a with EXPJ1 in Fig. 1a shows that the temperature differences with CAM2 have been reduced in EXPJ2,
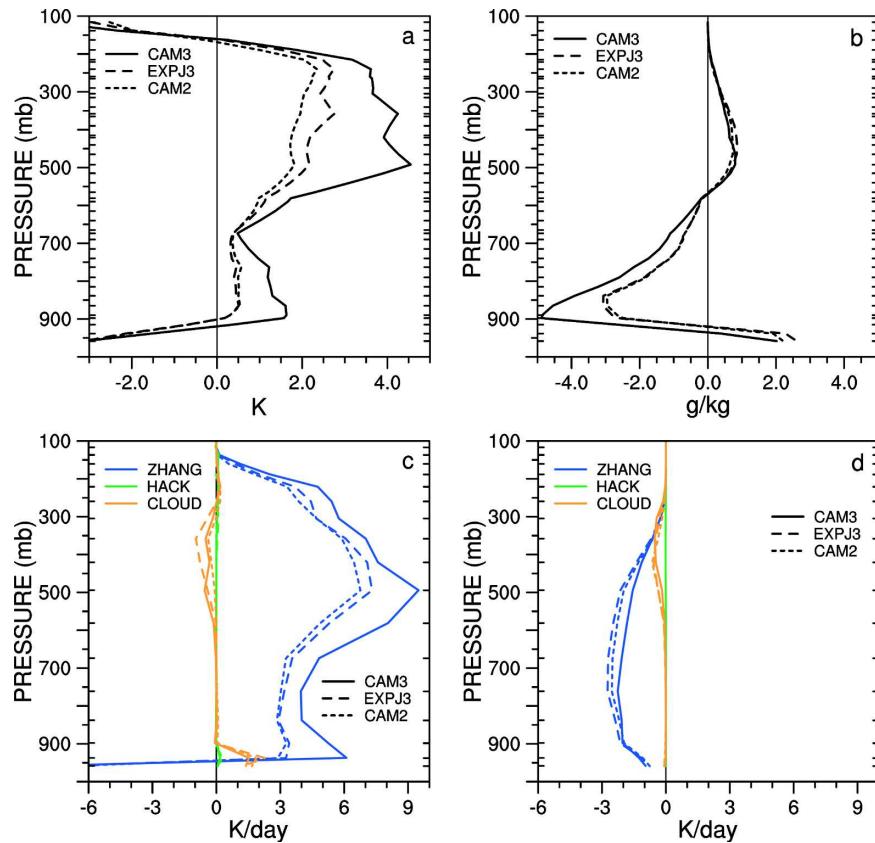
FIG. 5. Mean day-1 (a) forecast temperature and (b) specific humidity errors for CAM3, EXPJ3, and CAM2 for the June–July 1997 IOP. Mean forecast 0–24-h average temperature tendencies from (c) formation of condensate and (d) rainfall evaporation associated with Zhang–McFarlane deep convection (ZHANG), Hack shallow convection (HACK), and prognostic cloud parameterization (CLOUD).

especially in the upper troposphere. The moisture differences have been only slightly reduced in EXPJ2 in the lower troposphere (Fig. 4b versus Fig. 1b). Note that the phase conversion does not directly affect the atmospheric water vapor specific humidity. It only directly affects the temperature, and ice and liquid water components. The kink between 600 and 700 mb in the temperature error in CAM3 (Fig. 4a) is eliminated in EXPJ2. It was caused by the melting of falling snow, which led to localized cooling there (Fig. 3d). The difference in heating from the Zhang–McFarlane deep convection scheme (Fig. 4c) between CAM2 and EXPJ2 is rather small. The difference in temperature error however is not negligible. Between 900 and 200 mb the difference in temperature between EXPJ2 and CAM2 (Fig. 4a) is nearly constant. Similarly, the water vapor also shows a nearly constant difference from 900 to 500 mb (Fig. 4b), and that difference mimics the rainfall evaporation difference in temperature associated with the Zhang–McFarlane deep convection pa-

rameterization (Fig. 4d). Note that the corresponding water vapor tendencies from rainfall evaporation (not shown) are just the negative of the temperature tendencies scaled by the latent heat of vaporization.

Thus the last experiment in the series, EXPJ3, examines the contribution from the change in the rainfall evaporation formulation. A multiplicative term $(1 - C_f)$ that was included in CAM3 in the rainfall evaporation equation, where C_f is the cloud fraction, is eliminated in EXPJ3 [Eq. (4.103) of Collins et al. 2004]. Figure 5 shows the result of a series of forecasts from EXPJ3. Now the moisture error in EXPJ3 is very close to that of CAM2 (Fig. 5b) and the evaporation term itself is also very close to that of CAM2 (Fig. 5d). The temperature tendency from conversion of vapor to liquid in the Zhang–McFarlane deep convection scheme matches CAM2 well with slight differences around 500 mb (Fig. 5c). The temperature error itself shows differences with CAM2 of 0.5 K above 500 mb (Fig. 5a).

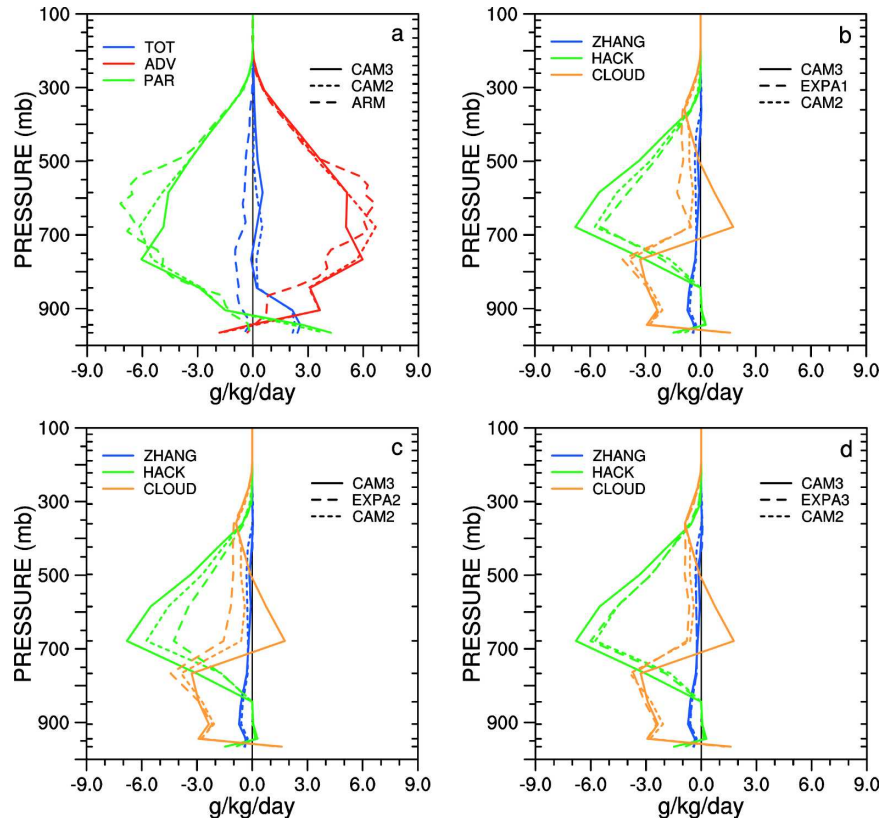At this point we have illustrated the effects of the

FIG. 6. Mean forecast 0–24-h average of terms in the specific humidity prediction equation for the April IOP for CAM3, ARM, and CAM2: (a) total (TOT), advection (ADV), and parameterization (PAR). Mean forecast 0–24-h average Zhang–McFarlane deep convection (ZHANG), Hack shallow convection (HACK), and prognostic cloud parameterization (CLOUD) specific humidity tendencies for (b) CAM3, EXPA1, and CAM2; (c) CAM3, EXPA2, and CAM2; and (d) CAM3, EXPA3, and CAM2.

primary changes that were responsible for the major differences between CAM3 and CAM2 in June–July 1997 at the SGP site. They are all associated with the Zhang–McFarlane deep convection parameterization. Small differences do however remain. Although we do not show it here, we have identified these as arising from changes in the prognostic cloud water and from the longwave radiation responding to changes in the cloud fraction parameterization. The cloud changes will be considered in the next section focusing on the April forecasts, where we also consider some of the prognostic cloud water differences. In the April case the prognostic cloud water and the Hack shallow convection parameterization are dominant and the Zhang–McFarlane deep convection is inactive.

4. April 1997 IOP forecasts

We now consider forecasts initialized in April 1997. Williamson et al. (2005) showed that unlike the summer case, in April the CAM2 captures the episodic nature of

the precipitation observed in ARM very well. The terms in the moisture and temperature prediction equations are very different on rain and no rain days. Therefore, for the April forecasts we consider composites of days with significant precipitation. The compositing is done here exactly as it was done in Williamson et al. (2005). Again, all members of the composite exhibit very similar forecast errors. We do not compare the composite forecast temperature and moisture errors with the model-simulated climate error as we did in July since the composite represents only a small sample of states composing the climate.

Figure 6a shows the vertical profiles of the 0–24-h average total moisture tendency along with its two components, advection and parameterization for CAM3 (solid line) and CAM2 (short dashed line). The long dashed line shows the ARM estimates from the variational analysis. The total tendency is very similar in CAM2 and CAM3, but both are different from ARM as discussed in Williamson et al. (2005) for CAM2.

TABLE 2. Sequence of experiments for April 1997 with accumulated changes from CAM3 back to CAM2.

EXPA1	CAM3 without convective detrainment of liquid water associated with the Hack parameterization
EXPA2	EXPA1 with Hack convective time scale set to CAM2 value
EXPA3	EXPA2 with cloud fraction scheme converted to CAM2 scheme

Since the two model tendencies are very similar it naturally follows that the errors at day 1 are very similar. The error for CAM2 can be seen in Fig. 5 of Williamson et al. (2005). Although the temperature and moisture errors in CAM2 and CAM3 are very similar, we will show in the following that when one parameterization is modified from its CAM3 form to its CAM2 form, there are compensating responses in the dynamics or in another parameterization that lead to the same total errors in the two models.

We illustrate these compensating responses with a sequence of experiments changing CAM3 back toward CAM2 summarized in Table 2. The changes to create CAM3 from CAM2 and their observed compensating responses are 1) the addition of detrainment of water in CAM3 by the Hack shallow convection to the prognostic cloud water scheme, which is balanced by a resulting difference in the advective tendency, 2) a halving of the time scale assumed for the Hack shallow convection, which is compensated by a resulting change in the prognostic cloud water, and 3) changes to the cloud fraction parameterization that affect the radiative heating. This in turn modifies the stability of the atmospheric column and affects the convection. The resulting changes in convection tendency are balanced by responding changes in the prognostic cloud water parameterization tendency.

Figure 6a shows that the two components of the total tendency, advection (ADV) and parameterizations (PAR), are very similar in CAM2 and CAM3 except at a single grid level (675 mb) where a compensating decrease occurs in both ADV and PAR in CAM3 compared to CAM2, taking each farther from the ARM estimates. Since the advection approximations are identical in CAM2 and CAM3, and since the initial conditions are also the same in the two experiments, the advection difference is probably a reflection of different heating rates produced by the different parameterizations in the two models as was argued above for the July case. Above 900 mb the parameterizations in CAM2 are dominated by the moist processes (Williamson et al. 2005). As might be expected, this is also the case in CAM3.

Figure 6b shows the tendencies of the three primary parameterizations composing the moist processes for CAM3 and CAM2. The tendencies from the associated rainfall evaporations contribute little to the total moist process tendencies at this column and therefore are not included in the figure [see Fig. 6d of Williamson et al. (2005) for CAM2 curves.] The Hack shallow convection (green curves) generally has stronger drying in CAM3 than in CAM2, while the prognostic cloud parameterization (yellow curves) shows less drying in CAM3 than in CAM2, turning to moistening at the 675-mb grid level in CAM3. The differences in the tendencies of the two components compensate in most of the troposphere except at the two grid levels above 700 mb where the prognostic cloud water parameterization is moistening the atmosphere in CAM3. The prognostic cloud water scheme is a vapor source there in CAM3 but not in CAM2. Thus some other process in CAM3 is providing liquid water to the prognostic cloud water scheme, which is then available for evaporation. From the cloud liquid water budget we determined that detrainment of water by the Hack shallow convection to the prognostic cloud water scheme was the liquid source in CAM3. That process was not included in CAM2.

Experiment EXPA1 eliminates this detrainment from CAM3. Figure 6b includes the terms from EXPA1 as the long-dash line. The prognostic cloud parameterization tendency (yellow line) is negative everywhere above the first model level. In fact both the Hack shallow convection and the prognostic cloud water tendencies in EXPA1 are very similar to those of CAM2. This leads to the total moist parameterization tendencies for CAM2 and EXPA1 also being very similar (not shown). The advection tendency in EXPA1 (not shown) is also very similar to that of CAM2, yielding a similar total moisture tendency. The advection tendency is responding to the different prognostic cloud water tendency.

Although with this one change the total moist process and the primary parameterization tendencies now match CAM2 closely, there are other significant changes from CAM2 to CAM3 that affect the model behavior and balances. The adjustment time scale of the Hack shallow convection was decreased from 60 to 30 min in CAM3. Figure 6c shows the terms from EXP2, which is based on EXP1 but with the time scale of the Hack shallow convection parameterization increased from 30 to 60 min to match CAM2. The increased time scale results in a decrease in the Hack shallow convective tendency so that it is now smaller
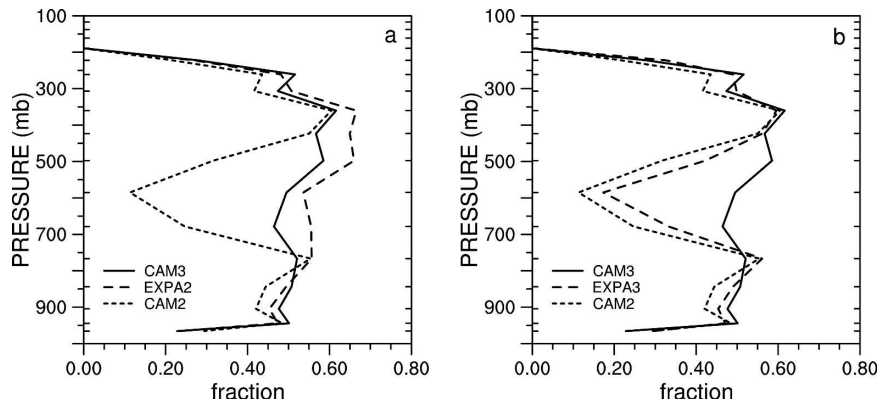
FIG. 7. Mean forecast 0–24-h average cloud fraction for (a) CAM3, EXPA2, and CAM2 and (b) CAM3, EXPA3, and CAM2.

than that of CAM2, which in turn was smaller than CAM3. This difference between EXPA1 and EXPA2 in the Hack shallow convection parameterization tendency is balanced by an opposing difference in the prognostic cloud water tendency, which now has greater drying than that of CAM2. Although the Hack shallow and prognostic cloud water tendencies each differ between EXPA2 and CAM2 (Fig. 6c), the total moist parameterization tendency (not shown) agrees rather well between EXPA2 and CAM2 as it did in the previous experiment (EXPA1). Once again, a change made to one component leads to a compensating response in another that results in a very similar net drying.

Although the total moist tendencies of EXPA2 and CAM2 agree well, Fig. 6c shows that the individual components do not. The remaining differences are attributable to a packet of changes in the cloud fraction scheme and responses of other parameterizations to those changes. EXPA3 removes these changes from EXPA2. This results in forecasts in which the moist parameterization component tendencies match those of CAM2 (Fig. 6d) as does the total moist parameterization tendency itself (not shown). The packet of changes to the cloud fraction scheme includes the following: the minimum relative humidity for low stable clouds was changed from 85% in CAM2 to 90% in CAM3 while that for high stable clouds was changed from 90% in CAM2 to 80% in CAM3. The low cloud value is effective below 750 mb and the high cloud above 750 mb. CAM2 convective cloud fraction depends on the detrainment rate from deep convection, while that of CAM3 depends on the convective mass flux. Finally in CAM2 the total cloud fraction is the maximum of the stable and convective cloud fractions (maximum overlap), while in CAM3 the total cloud is the sum of the stable and convective cloud fractions.

In EXPA3, without the CAM3 cloud fraction modifications, the midlevel cloud fraction is seen to be less than that of CAM3 (Fig. 7b), while with them (EXPA2) the fraction is closer to that of CAM3 (Fig. 7a). In fact a design goal of CAM3 was to increase the midlevel clouds over those of CAM2. The decreased midlevel clouds in EXPA3 (relative to CAM3 and EXPA2) results in increased longwave cooling below 600 mb extending down to 850 mb (not shown). The shortwave radiation heating is affected less by these clouds so the net radiation has increased cooling in EXPA3 relative to CAM3 and EXPA2 from 600 to 800 mb. That destabilizes the atmosphere leading to stronger convection in EXPA3, which then matches CAM2 in drying.

EXPA3 is very close to CAM2 in the total moist parameterization drying (not shown), in the moist parameterization components (Fig. 6d), and in the cloud fraction (Fig. 7b). Small subtle differences do remain but we do not try to identify their causes. Our goal was to determine which model formulation changes had the largest effects.

5. Conclusions

The studies described in the introduction have shown that the simulated climate of CAM3 matches similar statistics obtained from atmospheric observations and analyses better than the simulated climate of its predecessor CAM2 does. With that measure CAM3 represents a significant improvement over CAM2. However, to be most useful a climate model must not only simulate the correct statistics, but it must do so by correctly modeling the relevant processes. The comparison of CAM3 with CAM2 in this paper attempts to examine the modeled processes that create the climates of the models by examining the models applied to weather

forecasts. We compare the global model forecast evolution to estimates of that evolution at the ARM SGP site for several IOPs. For such comparisons we are limited to specific locations and periods. With these limited locations and periods we can only sample a small set of the phenomena that make up the global climate of the model. We compute the model errors by comparing with the ARM constrained variational analysis (Zhang and Lin 1997; Zhang et al. 2001) that was developed to drive and analyze single-column models.

We isolated the primary model changes from CAM2 to CAM3 that affect the simulated forecast processes and errors. There are significant differences in the errors in forecasts made with CAM3 and CAM2 at the ARM SGP site in June–July 1997. In April 1997 the temperature and moisture forecast errors are quite similar, but the individual components that combine to yield the total error can be quite different in compensating ways. We performed a series of experiments to illustrate the changes in the model formulation that were responsible for the major changes in the errors and balances. Many smaller, more subtle changes were not pursued.

In June–July 1997 the CAM3 temperature and moisture forecast errors were in fact larger than those of CAM2 at this SGP site. We concentrated on the temperature balance terms as they include terms from the phase change between liquid water and ice that have no direct effect on the water vapor itself. The changes identified as being responsible for the differences were 1) the deep convection was made more active in CAM3 by halving the assumed time scale and increasing the autoconversion coefficient, 2) including the energy associated with the conversion between water and ice of the Zhang–McFarlane rain in CAM3, and 3) adding a dependence of the rainfall evaporation on cloud fraction in CAM3. These last two were not included in CAM2.

In April 1997 the CAM3 and CAM2 forecast temperature and moisture forecast errors were very similar, yet when certain parameterization components were modified, other components reacted in a compensating way. We examined the water vapor balance terms in detail. The detrainment of water by the Hack shallow convection to the prognostic cloud water scheme that was included in the CAM3 led to a different total parameterization tendency from that of CAM2, but this difference was balanced by a compensating change in the advective tendency to yield the same total moisture tendency. The convective time scale assumed for the Hack shallow convection was halved in CAM3. Thus the convection tendency was weaker in CAM2 but compensated by the prognostic cloud water parameter-

ization tendency, which responded to give very similar total parameterization tendencies. CAM3 also had a variety of changes to the cloud fraction parameterization. These affect the radiative heating, which in turn modifies the stability of the atmospheric column and affects the convection. But again, the resulting difference in convection tendency that arises from the different stability was balanced by responses in the prognostic cloud water parameterization tendency, yielding a similar total parameterization tendency.

Except for the detrainment of water by the Hack shallow convection, the other two modifications to the parameterizations from CAM2 to CAM3 studied here in the April case each led to compensating changes between the tendencies from the Hack shallow convection parameterization and the prognostic cloud water parameterization. In other words, several different parameter settings lead to the same net tendency, but distributed differently among potentially competing processes. Such compensation is disturbing since it makes it even harder to establish if the processes are correct. It indicates the need for more observations to establish which parameter setting is correct, that is, to tie down parameters in each component. Of course we cannot observe individual processes as formulated in the model, but other variables such as clouds might help. Or perhaps the parameterizations should not be considered as individual processes but unified in some manner that is still cost effective to solve. These are all examples of the delicate balance that determines the model climate. They indicate why it is important for each process to be modeled correctly if the model is to be applied to climate change studies.

Although the analysis presented here was performed after the fact in the model development process, it illustrates that this type of analysis would have been useful during the development phase. Based on the findings here different modifications might have been sought in the development cycle. For example, alternatives to the changes in convective time scales or the details of rainfall evaporation might have been sought that lead to the same improvements in the climate statistics but do not increase the temperature and moisture forecast errors. Clearly, however, basing development decisions solely on the two periods studied here at an individual model column would be dangerous. A large number of cases covering all phenomena being simulated by a climate model is needed. Then the trade-offs required in specifying the details of any model can be considered more logically and systematically.

REFERENCES

Bonan, G. B., S. Levis, L. Kergoat, and K. W. Oleson, 2002a: Landscapes as patches of plant functional types: An integrating concept for climate and ecosystem models. *Global Biogeochem. Cycles,* **16,** 1021, doi:10.1029/2000GB001360.

——, K. W. Oleson, M. Vertenstein, S. Levis, X. Zeng, Y. Dai, R. E. Dickinson, and Z.-L. Yang, 2002b: The land surface climatology of the Community Land Model coupled to the NCAR Community Climate Model. *J. Climate,* **15,** 3123–3149.

Boville, B. A., P. J. Rasch, J. J. Hack, and J. R. McCaa, 2006: Representation of clouds and precipitation processes in the Community Atmosphere Model Version 3 (CAM3). *J. Climate,* **19,** 2184–2198.

Boyle, J. S., D. Williamson, R. Cederwall, M. Fiorino, J. Hnilo, J. Olson, T. Phillips, G. Potter, and S. Xie, 2005: Diagnosis of Community Atmospheric Model 2 (CAM2) in numerical weather forecast configuration at Atmospheric Radiation Measurement (ARM) sites. *J. Geophys. Res.,* **110,** D15S15, doi:10.1029/2004JD005042.

Collins, W. D., and Coauthors, cited 2003: Description of the NCAR Community Atmosphere Model (CAM2). [Available online at http://www.ccsm.ucar.edu/models/atm-cam/docs/cam2.0.]

——, and Coauthors, 2004: Description of the NCAR Community Atmosphere Model (CAM3.0). NCAR Tech. Note NCAR/TN-464+STR, xii+214 pp.

——, and Coauthors, 2006a: The Community Climate System Model: CCSM. *J. Climate,* **19,** 2122–2143.

——, and Coauthors, 2006b: The formulation and atmospheric simulation of the Community Atmosphere Model Version 3 (CAM3). *J. Climate,* **19,** 2144–2161.

Hack, J. J., 1994: Parameterization of moist convection in the National Center for Atmospheric Research community climate model (CCM2). *J. Geophys. Res.,* **99,** 5551–5568.

——, J. M. Caron, G. Danabasoglu, K. W. Oleson, C. M. Bitz, and J. E. Truesdale, 2006a: CCSM CAM3 climate simulation sensitivity to shanges in horizontal resolution. *J. Climate,* **19,** 2267–2289.

——, ——, S. G. Yeager, K. W. Oleson, M. M. Holland, J. E. Truesdale, and P. J. Rasch, 2006b: Simulation of the Global Hydrological Cycle in the CCSM Community Atmosphere Model Version 3 (CAM3): Mean features. *J. Climate,* **19,** 2199–2221.

Holtslag, A. A. M., and B. A. Boville, 1993: Local versus nonlocal boundary-layer diffusion in a global climate model. *J. Climate,* **6,** 1825–1842.

Hurrell, J. W., J. J. Hack, A. Phillips, J. Caron, and J. Yin, 2006: The dynamical simulation of the Community Atmosphere Model Version 3 (CAM3). *J. Climate,* **19,** 2162–2183.

Kanamitsu, M., W. Ebisuzaki, J. Woollen, S.-K. Yang, J. J. Hnilo, M. Fiorino, and G. L. Potter, 2002: NCEP-DOE AMIP-II reanalysis (R-2). *Bull. Amer. Meteor. Soc.,* **83,** 1631–1643.

Kiehl, J. T., and P. R. Gent, 2004: The Community Climate System Model, version 2. *J. Climate,* **17,** 3666–3682.

Oleson, K. W., and Coauthors, 2004: Technical description of the Community Land Model (CLM). Tech. Rep. NCAR/TN-461+STR, National Center for Atmospheric Research, 174 pp.

Phillips, T. J., and Coauthors, 2004: Evaluating parameterizations in general circulation models: Climate simulation meets weather prediction. *Bull. Amer. Meteor. Soc.,* **85,** 1903–1915.

Rasch, P. J., and J. E. Kristjansson, 1998: A comparison of the CCM3 model climate using diagnosed and predicted condensate parameterizations. *J. Climate,* **11,** 1587–1614.

——, and Coauthors, 2006: A characterization of tropical transient activity in the CAM3 atmospheric hydrologic cycle. *J. Climate,* **19,** 2222–2242.

Simmons, A. J., and J. K. Gibson, 2000: The ERA-40 project plan. ERA-40 Project Report Series 1, ECMWF, Reading, United Kingdom, 62 pp.

Sud, Y. C., D. M. Mocko, and S. J. Lin, 2006: Performance of two cloud-radiation parameterization schemes in the finite volume general circulation model for anomalously wet May and June 2003 over the continental United States and Amazonia. *J. Geophys. Res.,* **111,** D06201, doi:10.1029/2005JD006246.

White, P. W., Ed., 2001: FULL-POS postprocessing and interpolation. IFS Documentation, Part VI, Technical and Computational Procedures (CY23R4), ECMWF. [Available online at http://www.ecmwf.int/research/ifsdocs_old/TECHNICAL/index.html.]

Williamson, D. L., J. Boyle, R. Cederwall, M. Fiorino, J. Hnilo, J. Olson, T. Phillips, G. Potter and S. C. Xie, 2005: Moisture and temperature balances at the ARM Southern Great Plains Site in forecasts with the CAM2. *J. Geophys. Res.,* **110,** D15S16, doi:10.1029/2004JD005109.

Zhang, G. J., and N. A. McFarlane, 1995: Sensitivity of climate simulations to the parameterization of cumulus convection in the Canadian Climate Centre general circulation model. *Atmos.–Ocean,* **33,** 407–446.

Zhang, M. H., and J. L. Lin, 1997: Constrained variational analysis of sounding data based on column-integrated budgets of mass, heat, moisture, and momentum: Approach and application to ARM measurements. *J. Atmos. Sci.,* **54,** 1503–1524.

——, ——, R. T. Cederwall, J. J. Yio, and S. C. Xie, 2001: Objective analysis of ARM IOP data: Method and sensitivity. *Mon. Wea. Rev.,* **129,** 295–311.

——, W. Lin, C. S. Bretherton, J. J. Hack, and P. J. Rasch, 2003: A modified formulation of fractional stratiform condensation rate in the NCAR Community Atmosphere Model (CAM2). *J. Geophys. Res.,* **108,** 4035, doi:10.1029/2002JD002523.